Pyridine-Ring Alkylation of Cytotoxic *r*-1,*c*-3,*c*-5-Tris[(2-pyridylmethyl)-amino]cyclohexane Chelators: Structural and Electronic Properties of the Mn^{II}, Fe^{II}, Ni^{II}, Cu^{II} and Zn^{II} Complexes

Matt L. Childers,[a] Fan Su,[a] Ann M. Przyborowska,[a] Bimjhana Bishwokarma,[a] Gyungse Park,[a][‡] Martin W. Brechbiel,[b] Suzy V. Torti,[c] Frank M. Torti,[c] Grant Broker,[d] Jacob S. Alexander,[e] Robin D. Rogers,[d] Karin Ruhlandt-Senge,[e] and Roy P. Planalp*[a]

Dedicated to Prof. Dr. Heinrich Vahrenkamp on the occasion of his 65th birthday

Keywords: Antitumor activity / Tripodal ligands / Ligand design / Iron / Zinc / Copper

Effects of pyridyl-ring alkylation on complexation of Mn^{II}, Fe^{II}, Ni^{II}, Cu^{II} and Zn^{II} by chelators based on *r*-1,*c*-3,*c*-5-triaminocyclohexane (tach) have been studied. The chelators studied are *N*,*N*′,*N*′′-tris[(*x*-alkyl-2-pyridyl)methyl] derivatives of tach, where the ring substituents are 3-Me, 4-Me, 5-Me, 6-Me or 6-MeO ("tach-*x*-Rpyr"). Dicationic complexes were synthesized for most combinations of the above five metals and five chelators, using ClO_4^-, NO_3^-, Cl^-, or $CF_3SO_3^-$ as counterions. Their bonding, structure, and aqueous lability were analyzed by UV/Vis/NIR spectroscopy, magnetic moment determination, HPLC, and single-crystal X-ray crystallography. The striking features are seen in the 6-alkylated complexes, where steric repulsions between the 6-substituents at the threefold axis of the pseudo-octahedral coordination sphere result in a substantially weakened metal–ligand interaction. In the $[M(tach\text{-}6\text{-}Rpyr)]^{2+}$ series of divalent Mn, Ni, Cu and Zn, effects of these repulsions include bond angle and length distortions, decrease of the coordination number to five, shifts of d-d electronic transitions to lower energies, and spin-free complexes of the bound metal ion. Aqueous lability studies by HPLC agree with the spectroscopic findings. The bonding properties of the other tach-*x*-Mepyr chelators (x = 3, 4, 5) closely resemble the unalkylated parent tachpyr in solution. Similarly in the X-ray studies, $[Zn(tach\text{-}3\text{-}Mepyr)]^{2+}$ resembles $[Zn(tachpyr)]^{2+}$. The cytotoxicities of the chelators toward human breast cancer cells (MCF7) at a fixed chelator concentration of 16 μM show time-dependent induction of cell death in the order tach-3-Mepyr $>\approx$ tach-4-Mepyr $>$ tach-5-Mepyr $>$ tachpyr, whereas tach-6-Mepyr and tach-6-MeOpyr had no effect on the cells. The depressed cytotoxicities of the latter two are attributed to inability to bind Fe^{II} or Zn^{II} strongly.

Introduction

The tripodal aminopyridyl chelator tachpyr {*r*-1,*c*-3,*c*-5-tris[(2-pyridylmethyl)amino]cyclohexane} has been shown to readily complex divalent 3d transition metal ions;[1–4] tachpyr and its derivatives are under consideration as chemotherapeutic agents.[5–7] It is strongly cytotoxic to a variety of tumor cells as seen by an IC_{50} of 4.8 μM toward cultured bladder tumor cells. It is also preferentially toxic, showing a sevenfold decrease in IC_{50} in cancer cells relative to normal cells.[8] We have recently shown that it binds Zn^{II} and Fe^{II} in cells, and that the binding of Fe^{II} in vitro is accompanied by redox processes.[9] Metal complexes are well known to promote oxidative damage by catalyzing production of $HO^{\cdot}$, $O_2^{\cdot-}$, or other species collectively termed reactive oxygen species (ROS). We therefore pursue the hypotheses that tachpyr may affect cells by causing depri-

[‡] Current address: School of Science and Technology, Kunsan National University,
68, Miryong-Dong, Kusan, Jeollabuk-Do, Republik of Korea 573-701
[a] Department of Chemistry, University of New Hampshire, Durham, NH 03824-3598, USA
Fax: + 603-862-4278
E-mail: roy.planalp@unh.edu
[b] Radiation Oncology Branch, National Institutes of Health, Bethesda, MD 20892, USA
[c] Departments of Biochemistry and Cancer Biology and the Comprehensive Cancer Center, Wake Forest University Health Sciences,
Winston-Salem, NC 27157, USA
[d] Department of Chemistry, The University of Alabama, Tuscaloosa, AL 35487, USA
[e] Department of Chemistry, Syracuse University, Syracuse, NY 13244, USA
Supporting information for this article is available on the WWW under http://www.eurjic.org or from the author.

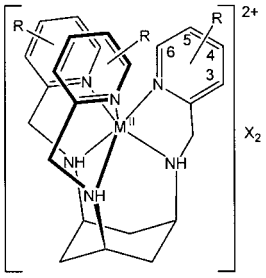

M(II)	tach-3-Mepyr (R = Me)	tach-4-Mepyr (R = Me)	tach-5-Mepyr (R = Me)	tach-6-Mepyr (R = Me)	tach-6-MeOpyr (R = MeO)	tachpyr (R = H)
Mn(II)	–	–	–	**1d** (X=ClO_4^-) **1d'** (X=$CF_3SO_3^-$)	**1e** (X=$CF_3SO_3^-$)	–
Fe(II)[a]	**2a**	**2b**	**2c**	**2d** (X=ClO_4^-)	**2e**	–
Ni(II)[b]	**3a**	**3b**	**3c**	**3d** (X= ClO_4^-) **3d'** (X= NO_3^-)	**3e**	–
Cu(II)[b]	**4a**	**4b**	**4c**	**4d**[3]	**4e**	–
Zn(II)[c]	**5a**	**5b**	**5c**	**5d** (X=NO_3^-) **5d'** (X=ClO_4^-)	**5e**	**5f** (X=$CF_3SO_3^-$)

[a] X = Cl^-(except **2d**); [b] X = ClO_4^- (except **3d'**); [c] X = NO_3^- (except **5d'** and **5f**)

Scheme 1. Structures and numbering of the isolated metal complexes of tach-*x*-Mepyr and tach-6-MeOpyr.

vation of essential biometals and/or that the complexes formed may go on to catalyze oxidative damage, particularly those of redox-active bioavailable metals such as Fe and Cu.

Study of pyridyl-ring-alkylated tachpyr variants appeared appropriate in order to change electronic properties or induce steric hindrance in tachpyr and its derivatives. Herein we focus on the ability of such derivatives to bind divalent biometals as seen from the coordination geometries and the electronic properties of $[M^{II}(tach\text{-}x\text{-}Rpyr)]^{2+}$ (Scheme 1; M = Mn, Fe, Ni, Cu, Zn; R = Me where x = 3–6 and R = MeO where x = 6). The electronic structure in solution has been studied by spectroscopy, and solid-state structures have been studied by single-crystal X-ray crystallography. Aqueous formation processes have been studied by electronic spectroscopy, and the lability of isolated complexes has been investigated by reversed-phase HPLC. Cytotoxicities of tach-*x*-Rpyr in human breast cancer (MCF7) cells are reported and the relationship of metal chelation to biological effects is discussed. In toxicity studies, tach-3-Mepyr, tach-6-Mepyr and tach-6-MeOpyr emerged as most interesting, tach-3-Mepyr due to more rapid onset of toxicity and the tach-6-Rpyr derivatives due to lack of toxicity, hence, these have received greater scrutiny in the present work.

Results and Discussion

Complexation Processes and Products

To investigate steric and electronic effects resulting from variation of the metal ion in the series **1*x***, **2*x***, **3*x***, **4*x*** and **5*x*** and of chelator in the series **#a**, **#b**, **#c**, **#d**, **#e** (Scheme 1), binding of Mn^{II}, Fe^{II}, Ni^{II}, Cu^{II}, and Zn^{II} by tach-*x*-Mepyr (x = 3, 4, 5, and 6) and tach-6-MeOpyr was studied in aqueous and nonaqueous solution. Isolation of complexes proceeded straightforwardly in MeOH by reaction of equimolar amounts of ligands and metal ion salts of counterions Cl^-, ClO_4^-, NO_3^- and $CF_3SO_3^-$ followed by precipitation with Et_2O. The counterion ClO_4^- provided superior material for X-ray study, while the other counterions were preferred for most solution studies due to greater aqueous solubility. Due to the ability of Fe^{II} to mediate oxidation of bound tachpyr,[2] all studies with this metal ion were conducted under anaerobic conditions. To study solution chemistry of alkylated tach chelators, complexation of Fe^{II}, Ni^{II}, Cu^{II} and Zn^{II} ions was carried out generally in water (for all tach-3-Mepyr and tach-6-Mepyr cases and most others; MeOH for a few cases) and the resulting solutions were analyzed. Adequate concentrations for analysis, ca. 5×10^{-2} M were obtained with all counterions except ClO_4^-. The appropriate physical methods were employed including UV/Vis/NIR spectroscopy, ^1H NMR spectroscopy, HPLC and solution magnetic moment determination. The electronic spectra from solution complexation closely resembled those of isolated complexes **2a**–**4e** in MeCN (Table 1 and Exp. Sect.). Mn^{II} complexation was generally not possible in aqueous media, and tach-6-Mepyr complexes were labile under HPLC conditions in some cases (see below). The spectral analyses of the solutions were consistent with six-coordination in all cases except $[Cu(tach\text{-}6\text{-}MeOpyr)]^{2+}$ which is discussed later.

HPLC studies provided good qualitative indications of lability trends and lipophilicities as a function of chelator and metal ion. The method very clearly distinguished metal

Table 1. UV/Vis/NIR spectroscopic data for tach-*x*-Mepyr complexes.[a]

Complex	ν [cm^{-1}][a]	Assignments[b]	Δ_o [cm^{-1}]	Color
[Fe(tach-3-Mepyr)]Cl_2	22700 (7000)	MLCT	–	bronze
	18200 sh (290)	$^1A_{1g} \rightarrow {}^1T_{1g}$		
[Fe(tach-4-Mepyr)]Cl_2	23100 (6600)	MLCT	–	bronze
	17800 sh (320)	$^1A_{1g} \rightarrow {}^1T_{1g}$		
[Fe(tach-5-Mepyr)]Cl_2	22600 (4200)	MLCT	–	bronze
	17400 sh (290)	$^1A_{1g} \rightarrow {}^1T_{1g}$		
[Fe(tach-6-Mepyr)]$(ClO_4)_2$	28800 (650)	MLCT		
	19600 sh (36.6)	unassigned	11700	red-
	11700 (9.4)	$^5T_{2g} \rightarrow {}^5E_g$		brown
[Fe(tach-6-MeOpyr)]Cl_2	28200 (790)	MLCT		
	11100 (5)	$^5T_{2g} \rightarrow {}^5E_g$	11100	yellow
[Ni(tach-3-Mepyr)]$(ClO_4)_2$	11300 sh (10.8)	$^3A_{2g} \rightarrow {}^1E_g$		
	12900 (15.9)	$^3A_{2g} \rightarrow {}^3T_{2\,g}$	12900	pink
	19700 (11.7)	$^3A_{2g} \rightarrow {}^3T_{1g}$		
[Ni(tach-4-Mepyr)]$(ClO_4)_2$	11300 sh (12.7)	$^3A_{2g} \rightarrow {}^1E_g$		
	12800 (15.9)	$^3A_{2g} \rightarrow {}^3T_{2g}$	12800	pink
	19500 (14.2)	$^3A_{2g} \rightarrow {}^3T_{1g}$		
[Ni(tach-5-Mepyr)]$(ClO_4)_2$	11200 sh (12.7)	$^3A_{2g} \rightarrow {}^1E_g$		
	12800 (17.0)	$^3A_{2g} \rightarrow {}^3T_{2g}$	12800	pink
	19500 (14.2)	$^3A_{2g} \rightarrow {}^3T_{1g}$		
[Ni(tach-6-Mepyr)]$(ClO_4)_2$	10800 (25.4)	$^3A_{2g} \rightarrow {}^3T_{2g}$		
	12400 sh (11.4)	$^3A_{2g} \rightarrow {}^1E_g$	10800	pale
	18100 (9.28)	$^3A_{2g} \rightarrow {}^3T_{1g}$		brown
[Ni(tach-6-MeOpyr)]$(ClO_4)_2$	10900 (17.5)	$^3A_{2g} \rightarrow {}^3T_{2g}$		
	12400 sh (11.4)	$^3A_{2g} \rightarrow {}^1E_g$	10900	violet
	18100 (7.28)	$^3A_{2g} \rightarrow {}^3T_{1g}$		
[Cu(tach-3-Mepyr)]$(ClO_4)_2$	15300 (97.1)	$^2E_g \rightarrow {}^2T_{2g}$	15300	blue
[Cu(tach-4-Mepyr)]$(ClO_4)_2$	15100 (88.3)	$^2E_g \rightarrow {}^2T_{2g}$	15100	blue
[Cu(tach-5-Mepyr)]$(ClO_4)_2$	15000 (68.8)	$^2E_g \rightarrow {}^2T_{2g}$	15000	blue
[Cu(tach-6-Mepyr)]$(ClO_4)_2$[3]	10800 (154.3)	$d_{xz,yz} \rightarrow d_{x^2-y^2}$	–	blue
	14100 (89.5)	$d_{xy} \rightarrow d_{x^2-y^2}$		
	15400 (223.8)	$d_{z^2} \rightarrow d_{x^2-y^2}$		
[Cu(tach-6-MeOpyr)]$(ClO_4)_2$	10400 (117.9)	$d_{xz,yz} \rightarrow d_{x^2-y^2}$	–	blue
	14100 (34.4)	$d_{xy} \rightarrow d_{x^2-y^2}$		
	15300 (174.5)	$d_{z^2} \rightarrow d_{x^2-y^2}$		

[a] All Fe^{II} and Ni^{II} complex spectra measured in MeCN; all Cu^{II} spectra measured in MeOH except [Cu(tach-6-Mepyr)]$(ClO_4)_2$ and [Cu(tach-6-MeOpyr)]$(ClO_4)_2$ which were measured in H_2O. [b] In the case of d-d transitions, assignments of pseudo-octahedral complexes are made in the O_h point group while the square-pyramidal Cu^{II} complexes are given as transitions between individual orbitals according to literature conventions.

complex from metal chelator and was particularly appropriate for study of Zn^{II} and Mn^{II} speciation where Vis/NIR spectroscopy is not available.[1,9] Due to their polarity the metal complexes eluted at 12 to 15 min, whereas free chelator retention times were upwards of 20 min. The separation was improved by isocratic elution with a mobile phase of 90% Et_3N/HOAc buffer and 10% MeOH in order to clearly discriminate complexes of different metal ions with the same chelator.

The Mn^{II} complexes **1d** and **1e** could be prepared in MeOH, but they dissociated completely under HPLC analysis, as expected given the poor match of size and hard–soft acid–base properties as well as the steric effects of 6-substitution of the coordinating pyridine ring. The $[Zn(tach\text{-}6\text{-}Mepyr)]^{2+}$ complex **5d** was also labile, but $[Zn(tach\text{-}3\text{-}Mepyr)]^{2+}$ (**5a**) and $[Zn(tachpyr)]^{2+}$ (**5f**) yielded clean single peaks, indicative of inertness.

Ring alkylation of tachpyr increased lipophilicity of chelators and complexes as shown by RP-HPLC studies in the gradient mode. Thus, the free chelator tachpyr and $[Zn(tachpyr)]^{2+}$ eluted at substantially shorter times (18.8 min and 8.4 min) than the respective alkylated compounds tach-3-Mepyr and $[Zn(tach\text{-}3\text{-}Mepyr)]^{2+}$ (22.9 min and 14.6 min).

^1H NMR spectra of complexes **2a**–**c** and **5a**–**e** are consistent with the octahedral-enforcing nature of tach-framework chelators as previously shown in $[Ni(tachpyr)]^{2+}$, $[Zn(tachpyr)]^{2+}$ and $[Ga(tachpyr)]^{3+}$.[4] Characteristic patterns of proton–proton coupling between cyclohexyl H atoms indicate "closed", complexed tach as opposed to "open" tach.[1] The two methylene protons of the coordinated pendant arms are diastereotopic, indicating that the arms of these complexes are twisted about the metal ion in the Δ or Λ configuration, and Δ–Λ interconversion does not occur on the NMR time-scale at room temperature, also as previously found for $[M(tachpyr)]^{2+}$ (M = Fe^{II}, Zn^{II}, Ga^{III}, In^{III}).[1,2,18]

In total, synthetic and physical studies demonstrate the alkylated derivatives of tachpyr to be effective chelators of Fe^{II}, Ni^{II}, Cu^{II} and Zn^{II}, while Mn^{II} is not bound in aqueous media, and some of the 6-alkylated tachpyr variants are labile in aqueous media.

Electronic Structure

To examine metal-complex structures in solution and assess effects of pyridyl substituents at various positions, the UV/Vis/NIR spectra of the Fe^{II}, Ni^{II}, and Cu^{II} complexes were measured, assigned, and compared with other amino/pyridyl–metal compounds (Table 1). The spectral assignments for Ni^{II} and Cu^{II} complexes were made as previously reported for their complexes of tachpyr and *N*-alkylated tachpyr derivatives.[1,3] The Fe^{II} complexes **2a**–**c** exhibit a large absorption band at 22600–23100 cm^{-1} with a weak low-energy shoulder at 17400–18200 cm^{-1}. We assign the intense absorption to a metal-to-ligand charge-transfer band ($d\pi \rightarrow p\pi^*$) typical of LS Fe^{II} complexes with π-acceptor ligands.[19–22] This absorption appears to mask all d-d transitions except the low-energy shoulder that is generally assigned as the $^1A_{1g} \rightarrow {}^1T_{1g}$ transition in LS Fe^{II} or Co^{III} complexes.[20,23]

Comparison across the chelate tach-*x*-Mepyr series shows that 6-substituted ligands have weaker field strength toward Fe^{II}, Ni^{II}, and Cu^{II}, while methyl substitution at the 3, 4, and 5 positions on the pyridine rings has no notable effect on the field strength relative to tachpyr. Thus, the 6-substituted Ni^{II} complexes **3d** and **3e** have lower d-d transition energies as compared to the 3-, 4- and 5-substituted compounds **3a**–**c**. In the Fe^{II} series, 6-substitution causes a shift of Fe^{II} from low-spin (LS) to high-spin (HS) state. The Fe^{II} complexes **2d** and **2e** contain a considerably weaker MLCT band around 28500 cm^{-1} with a slight shoulder to lower energy. The MLCT band is weaker as is typical for HS Fe^{II}.[20] Additionally there is a very weak absorption at 11100–11800 cm^{-1}. This absorption is assigned to a $^5T_{2g} \rightarrow {}^5E_g$ transition, as is seen in $[Fe([12]aneN_3py_3)]^{2+}$ and other HS Fe^{II} complexes.[19,20,22]

Alkylation of the pyridyl 6-position leads to a five-coordinate complex in the case of Cu^{II}. The UV/Vis/NIR spectrum of $[Cu(tach\text{-}6\text{-}MeOpyr)]^{2+}$ **4e** displays a low energy shoulder indicative of five-coordination as seen for $[Cu(tach\text{-}6\text{-}Mepyr)]^{2+}$ (**4d**).[3] We obtain a satisfactory fit to three Gaussian peaks (Figure 1) which we assign to the $d_{z^2} \rightarrow d_{x^2-y^2}$, $d_{xy} \rightarrow d_{x^2-y^2}$, and $d_{xy,yz} \rightarrow d_{x^2-y^2}$ transitions in order of increasing energy as has been shown for aqueous $[Cu(tach\text{-}Et_3)(H_2O)_2]^{2+}$ and other square-pyramidal Cu^{II} complexes.[24–26] The molar absorptivities of the component peaks are relatively high, ca. 25–160 M^{-1} cm^{-1} as is typical of d-d transitions of square-pyramidal copper complexes where parity-forbidden Laporte selection rules are relaxed by lowered symmetry.[27]

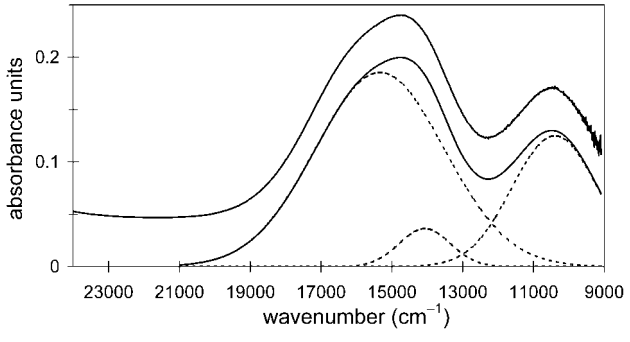

Figure 1. Resolution of the electronic spectrum of $[Cu(tach\text{-}6\text{-}MeOpyr)](ClO_4)_2$ (aq) into bands (L to R, dotted lines): $d_{xz,yz} \rightarrow d_{x^2-y^2}$, $d_{yz} \rightarrow d_{x^2-y^2}$ and $d_{z^2} \rightarrow d_{x^2-y^2}$. The calculated spectrum in the range 21000–9000 cm^{-1} is shown as a solid line and the experimental spectrum at 0.04 absorbance units above.

Overall, the weakened interactions between the 6-substituted ligands and the divalent metal centers that are seen here result in a substantially weakened ligand field as seen from coordination number, spin state, or d-d electronic transitions of the bound metal ion. The effects are due to steric hindrance produced by the methyl or methoxy groups when the pyridyl rings are brought into proximity in the closed conformation of the chelator.

Cytotoxicity Studies

The cytotoxicities of tach-*x*-Mepyr (*x* = 3–6) and of tach-6-MeOpyr were studied against a tachpyr control (Figure 2). Using a fixed concentration of chelator (16 μM), extent of cell death in the first 24 h varied considerably, whereas at the 72 h timepoint all chelators except tach-6-Mepyr and tach-6-MeOpyr had caused loss of 75–80% of cell viability. The lack of toxicity in the 6-substituted chelators is as expected because their metal-binding properties are sterically hindered as demonstrated by the solution UV/Vis spectra. However, there are significant differences in rate of cell killing, in the order tach-3-Mepyr $>\approx$ tach-4-Mepyr $>$ tach-5-Mepyr $>$ tachpyr. There is no corresponding variation in the ligand-field strength as a function of alkylated position on pyridine.

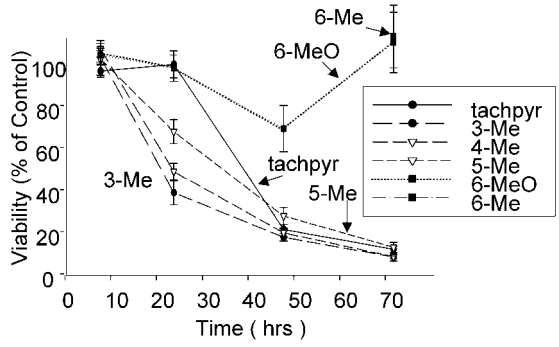

Figure 2. MCF7 cells were treated with 16 μM tach-*x*-Rpyr for the indicated times (8, 24, 48 and 72 h) and viability assessed using an MTT assay as described in Exp. Sect. Viability was expressed as percent survival relative to the control cells, which were untreated. Means and standard errors of 3 independent experiments are shown. In the case of 6-methyl-tachpyridine, only the 72 h timepoint was assessed.

Structural Studies

To elucidate the influences of the metal ion and alkylation of the pyridine rings of tachpyr upon bonding in the complexes, we undertook crystallographic studies of selected complexes. These studies focused on 6-alkylated and

Table 2. Selected structural parameters of tach-*x*-Rpyr complex cations and reference compounds.

	Metal ion radius [Å]	M–N(amine) bond distance or distance pairs[a] [Å]	M–N(pyridyl) bond distance or distance pairs[a] [Å]	Twist angle or angle pairs,[a] Φ [°]
$[Ni(tach\text{-}6\text{-}Mepyr)]^{2+}$	0.83	2.078(3) 2.099(3) 2.102(3)	2.191(3) 2.203(3) 2.267(3)	55.3(2)
$[Ni(tachpyr)]^{2+}$,[1]	0.83	2.099(4) 2.099(4) 2.107(4)	2.118(4) 2.122(4) 2.127(4)	45.5(2)
$[Cu(tach\text{-}6\text{-}MeOpyr)]^{2+}$	0.87	[2.051(3), 2.008(3)] [2.102(3), 2.045(3)] [2.170(3), 2.172(3)]	[1.994(3), 1.998(3)] [2.012(3), 2.093(3)]	–
$[Zn(tach\text{-}3\text{-}Mepyr)]^{2+}$	0.88	[2.151(3), 2.143(3)] [2.156(3), 2.163(3)] [2.167(3), 2.165(3)]	[2.156(4), 2.158(3)] [2.167(3), 2.170(3)] [2.170(3), 2.183(3)]	[42.8, 41.8]
$[Zn(tach\text{-}6\text{-}Mepyr)]^{2+}$	0.88	[2.128(4), 2.115(5)] [2.133(4), 2.133(5)] [2.135(4), 2.151(5)]	[2.203(4), 2.213(5)] [2.216(4), 2.218(5)] [2.566(5), 2.527(5)]	[53.9(3), 49.5(1)]
$[Zn(tachpyr)]^{2+}$,[4]	0.88	2.160(3) 2.160(3) 2.160(3)	2.165(4) 2.165(4) 2.165(4)	43.7(2)
$[Mn(tach\text{-}6\text{-}Mepyr)]^{2+}$	0.97	[2.235(3), 2.222(4)] [2.247(3), 2.258(3)] [2.262(3), 2.262(3)]	[2.277(3), 2.268(3)] [2.282(3), 2.289(4)] [2.442(3), 2.417(4)]	[52.6(3), 49.6(1)]
$[Mn(tach\text{-}6\text{-}MeOpyr)]^{2+}$	0.97	2.250(2) 2.286(2) 2.300(2)	2.210(2) 2.277(2) 2.306(2)	44.8(2)
$[Mn(tachpyr)]^{2+}$,[1]	0.97	2.2330(17) 2.236(2) 2.245(2)	2.2829(17) 2.2920(18) 2.2992(17)	2.5(1)

[a] In structures with two independent molecules per asymmetric unit, pairs of corresponding distances or angles are given in brackets.

3-alkylated pyridyl derivatives because of their particular influences on lability or biological activity. The salient findings are presented in Table 2, and views of selected complex cations are shown in Figures 3, 4, 5, 6 and 7.

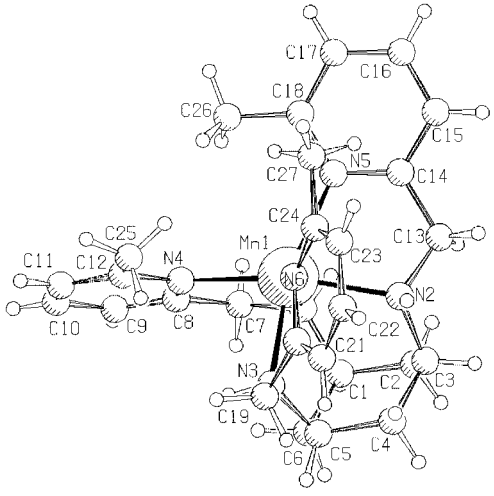

Figure 3. Projection along the N6–Mn bond of one cation in the asymmetric unit of $[Mn(tach\text{-}6\text{-}Mepyr)](ClO_4)_2\cdot 0.5H_2O\cdot 0.5MeOH$ (**1d**·$0.5H_2O$·0.5MeOH) (PLUTO) showing that the pyridyl ring C21•••C24 is not coplanar with the N6–Mn1 bond.

The M–N(amino) bond lengths of the complexes are generally comparable to the unalkylated analogues $[M(tachpyr)]^{2+}$ (M = Ni^{II}, Zn^{II}, Mn^{II})[1] and to other aminopyridyl ligands. They correlate well with the divalent metal ionic radii; as the six-coordinate ionic radius[28,29] increases from Ni^{II} (0.83 Å) to Zn^{II} (0.88 Å) to Mn^{II} (0.97 Å), the M–N bond lengths increase as well.

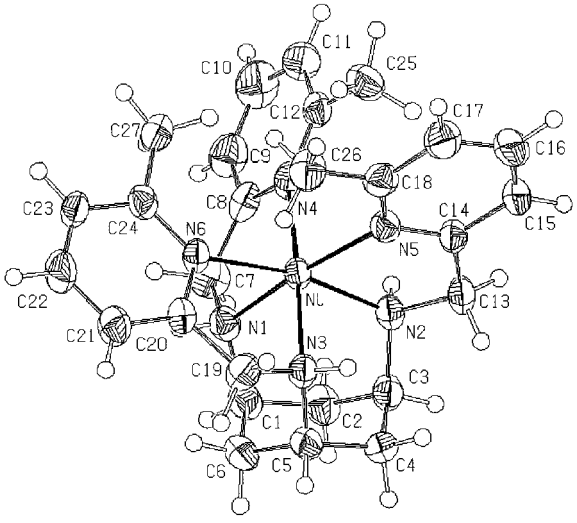

Figure 4. ORTEP view of the complex cation of $[Ni(tach\text{-}6\text{-}Mepyr)](NO_3)_2\cdot 0.5Et_2O$ (**3d′**·$0.5Et_2O$) (50% probability ellipsoids).

From the structural standpoint, 3-alkylation has little effect on complexation geometry in the solid state. The M–N bond lengths and the twist angle of $[Zn(tach\text{-}3\text{-}Mepyr)]^{2+}$ (**5a**) (Figure 6) are very comparable to those of $[Zn(tachpyr)]^{2+}$.[4]

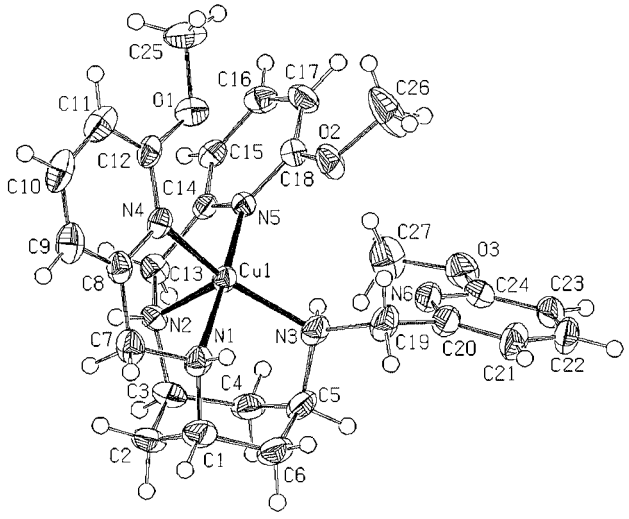

Figure 5. ORTEP view of one molecule in the asymmetric unit of $[Cu(tach\text{-}6\text{-}MeOpyr)](ClO_4)_2$ (**4e**) (50% probability ellipsoids).

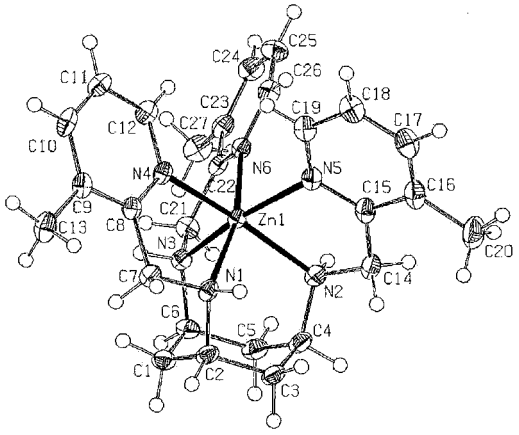

Figure 6. ORTEP view of one molecule in the asymmetric unit of $[Zn(tach\text{-}3\text{-}Mepyr)](NO_3)_2{\cdot}2MeOH{\cdot}0.5H_2O$ (**5a**·2MeOH·0.5H_2O) (50% probability ellipsoids).

However, the M–N(pyridyl) distances vary substantially in the 6-alkylated compounds. Elongations of the $Mn–N_{(py)}$ bond lengths due to steric hindrance may be uniform as seen in the cations $[Ni(tach\text{-}6\text{-}Mepyr)]^{2+}$ (**3d′**) (Figure 4) and $[Mn(tach\text{-}6\text{-}MeOpyr)]^{2+}$ (**1e**) or non-uniform as in $[Zn(tach\text{-}6\text{-}Mepyr)]^{2+}$ (**5d′**) (Figure 7) and $[Mn(tach\text{-}6\text{-}Mepyr)]^{2+}$ (**1d**) (Figure 3). The Ni^{II} complex **3d′** shows a uniform elongation (i.e., $Ni^{II}–N_{(py)}$ distances increase similarly) by roughly 0.11 Å relative to $[Ni(tachpyr)]^{2+}$ for all three $N_{(py)}$ donor atoms. In contrast, the Zn^{II} complex **5d′** shows two lesser elongations (ca. 0.050 Å) of the $Zn–N_{(py)}$ bonds and one very long bond with an elongation of ca. 0.38 Å. In the non-uniform elongation case, it is notable that the plane of the pyridyl ring is not coplanar with the longest $M^{II}–N_{(py)}$ bond; thus, the lone pair of the pyridyl N atom is directed away from the metal center. This is illustrated by a projection of $[Mn(tach\text{-}6\text{-}Mepyr)]^{2+}$ along the (longest) Mn1–N6 bond in Figure 3.

The compound $[Cu(tach\text{-}6\text{-}MeOpyr)](ClO_4)_2$ (**4e**) is five-coordinate in the solid state (Figure 5), consistent with the

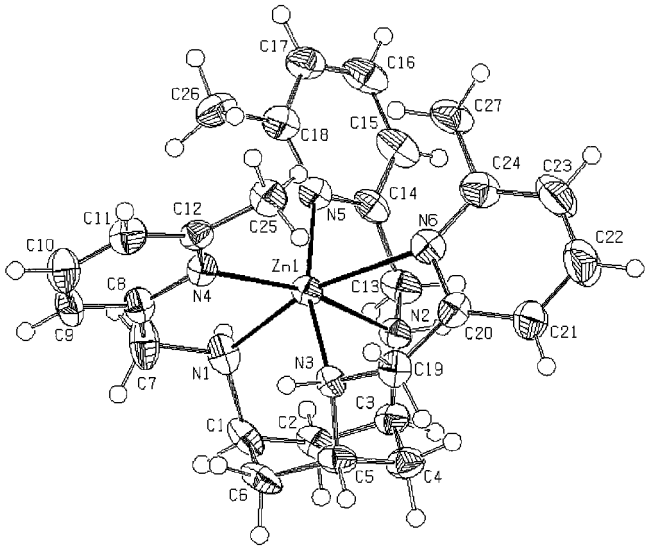

Figure 7. ORTEP view of one molecule in the asymmetric unit of $[Zn(tach\text{-}6\text{-}Mepyr)](ClO_4)_2{\cdot}0.5H_2O{\cdot}0.5MeOH$ (**5d′**·0.5H_2O·0.5MeOH) (50% probability ellipsoids).

assigned aqueous structure. This complex has four shorter bonds and one longer bond as expected in Jahn–Teller-distorted Cu^{II}, and previously observed in $[Cu(tach\text{-}6\text{-}Mepyr)](ClO_4)_2$ (**4d**).[3] The shorter bond lengths of **4e** [range 1.994(3) to 2.102(3) Å] compare favorably to those of **4d** [range 2.001(3)–2.103(3) Å] (Table 2), and the long distances [average of 2.171(3) Å in two molecules in the asymmetric unit] are somewhat shorter than in **4d** [2.216(3) Å]. Sterically crowded Cu^{II} is well known to assume coordination geometries varying from square-based pyramidal to trigonal-bipyramidal. In these cases the coordination geometry may be described by the in-plane angular distortion $\tau = (\beta - \alpha)/60°$, where β and α are the two basal angles formed by the *trans* ligands and the metal ion. The ideal square pyramid is defined by $\tau = 0$ and the trigonal bipyramid by $\tau = 1$.[30] The shape of Cu^{II} compound **4e** is closer to a square-based pyramid with an average $\tau = 0.26$ whereas **4d** has a more distorted intermediate shape, with $\tau = 0.58$.

In the case of Mn^{II}, the 6-substitution of the pyridyl ring makes the trigonal-prismatic geometry less favorable than distorted octahedral, as shown by comparison of trigonal twist angle (Φ) values in $[Mn(tach\text{-}6\text{-}Mepyr)]^{2+}$ (**1d**) and $[Mn(tach\text{-}6\text{-}MeOpyr)]^{2+}$ (**1e**) to $[Mn(tachpyr)]^{2+}$.[1] The Φ value is the angle by which the triangles of pyridyl N atoms and amino N atoms are staggered, as viewed down the pseudo-C_3 axis. The octahedron possesses perfect staggering with an angle $\Phi = 60°$ and the trigonal prism is perfectly eclipsed with $\Phi = 0°$. The value of Φ for $[Mn(tachpyr)]^{2+}$ is 2.5° while values of Φ for **1d** and **1e** are 52.6° and 44.8°, respectively. The drastic change in Φ reflects the closeness of 6-substituents to each other in a trigonal prism. It was observed in $[Mn(tachpyr)]^{2+}$ that extension of the pendant arms into a planar arrangement [i.e., making the N(H)–CH_2–(2-pyridyl) framework planar], to achieve a trigonal-prismatic coordination sphere, allowed the most favorable bite angles for a large metal ion. However, in the trigonal

prism the groups at the 6-pyridyl position must point directly at each other. Thus, **1d** and **1e** attain larger Φ values because sterics make the trigonal-prismatic geometry unfavorable in this case. Additionally, binding a metal ion into the trigonal-prismatic geometry of an aminopyridyl tach chelator causes severe distortions of the coordination geometry of the tach nitrogen atoms, forcing them into a trigonal-pyramidal geometry (with H at the apex of the pyramid).[1] In **1d** similarly to **5d**, the third arm is forced away from the other two at a greater Mn–N bond length, and it is unable to attain good overlap of the N(py) lone pair with Mn^{II} (Figure 3). In **1e**, steric effects do not seem as great, and the average N(py)–Mn bond length is marginally shorter than that of $[Mn(tachpyr)]^{2+}$ (Table 2).

Conclusions

The 6-position has a considerable effect on metal-binding properties in tach-6-Mepyr due to steric interactions amongst 6-substituents in metal-bound tach-6-Rpyr. On the other hand, there appears to be little electronic effect of 3-, 4-, or 5-alkylation on ligand-field strength in the tach-*x*-Mepyr series, nor any steric effect of 3-alkylation. The biological differences between tach-3-Mepyr and tachpyr appear to derive from other factors such as a difference in rate of metal ion binding, or formation constants of metal–ligand interaction, or other parameters specific to the Fe^{II} complexes. Studies of formation constants and complexation reactivities to compare the interactions of Zn^{II} and Fe^{II} with tach-3-Mepyr and tachpyr are therefore in progress.

Experimental Section

General: Full physical characterization of complexes was carried out with material prepared and isolated using nonaqueous solvents without optimization of yields. Aqueous complexation studies are described by a general procedure for each metal. X-ray crystallography was carried out on the isolated complexes from nonaqueous media. Cytotoxicity studies were performed with phosphate-buffered saline solutions of the free chelators, which were prepared as reported.[3,10]

Materials and Methods: All the materials cited below were of research grade or spectro-quality grade in the highest purity available and were generally obtained from commercial sources and used without further purification except Et_2O. Et_2O was distilled from Na and used immediately. $[D_6]$DMSO was obtained from Cambridge Isotope Laboratories. UV/Vis/NIR solution electronic spectra were measured using a Varian Cary 5 or a Varian Cary 50-Bio UV/Vis spectrometer with 1- or 3-mL quartz cuvettes (1 cm path length). Solid-phase Vis spectra were obtained with a model RSA-HP-53 reflectance spectroscopy attachment (Labsphere, Inc.) to an HP8453 diode-array instrument. All solution UV/Vis/NIR spectra are presented in Table 1; deconvolutions of Cu^{II} spectra were performed using Microcal Origin 6.0 software. Electrospray ionization (ESI) mass spectra in the positive ion detection mode were obtained with a Finnegan LCQ Classic instrument with dual optical Paul traps and Picoview nanospray source. Fast-atom bombardment mass spectra (FAB-MS) were taken with an Extrel 4000 instrument in the positive ion detection mode. Samples were desorbed from mixtures of DMSO and Magic Bullet ("MB"). Calculations from the program developed by Scientific Instrument Services (http://www.sisweb.com/cgi-bin/mass10.pl, accessed August 2, 2004) aided in assignment of peaks. ^{1}H NMR spectra were obtained using a Bruker AM360 instrument or a Varian Mercury 400 MHz instrument. Chemical shifts are reported in ppm on the δ scale relative to TMS. Magnetic moments were determined using Evans' method.[11] Elemental analysis was performed by Atlantic Microlabs (Atlanta, Georgia). Drying was accomplished in air or under reduced pressure (ca. 10^{-2} Torr) with a standard Schlenk line. All work with Fe^{II} was conducted with standard Schlenk or glovebox techniques under prepurified N_2 or Ar due to the oxidation sensitivity of the complexes.[12]

CAUTION: Perchlorate salts can be explosive and should be handled with care. No explosions occurred during the course of this work.

Metal Complex Syntheses

[Mn(tach-6-Mepyr)](ClO$_4$)$_2$·H$_2$O (1d·H$_2$O): A colorless solution of $Mn(ClO_4)_2{\cdot}6H_2O$ (0.0899 g, 2.48×10^{-4} mol) in MeOH (2 mL) was added to a pale yellow solution of tach-6-Mepyr (0.110 g, 2.48×10^{-4} mol) in MeOH (2 mL) affording yellow prisms suitable for X-ray diffraction (shown to be **1d**·1/2MeOH·1/2H$_2$O). The crystals were isolated and dried under reduced pressure giving a pale yellow solid. The solid was washed with MeOH (5 mL) and Et_2O (5 mL) and dissolved in MeCN followed by vapor-phase diffusion of Et_2O generating yellow prisms. The prisms were isolated and dried under reduced pressure affording a yellow solid in 73.9% yield (0.128 g, 1.83×10^{-4} mol). MS (ESI): m/z = 498 [M – 2 ClO_4^- – H^+], 598 [M – ClO_4]. μ_{eff} (DMSO, 25 °C) = 5.79 B.M. $C_{27}H_{38}Cl_2MnN_6O_9$ (715.15): calcd. C 45.26, H 5.35, N 11.73; found C 44.93, H 5.16, N 11.98.

[Mn(tach-6-Mepyr)](CF$_3$SO$_3$)$_2$ (1d′): A solution of $Mn(CF_3SO_3)_2{\cdot}6H_2O$ (0.083 g, 1.8×10^{-4} mol) in MeOH (2 mL) was added to a pale yellow solution of tach-6-Mepyr (0.079 g, 1.8×10^{-4} mol) in MeOH (2 mL) giving a pale yellow solution. Addition of dry Et_2O (20 mL) to this solution gave a pale-yellow oil that was isolated by decantation and triturated to a light tan powder with Et_2O (2 × 20 mL). The powder was dried under reduced pressure, then taken up in MeOH (3 mL) and subjected to vapor-phase diffusion of Et_2O to provide colorless prisms that were isolated and dried under reduced pressure affording a 46% yield (0.066 g, 8.3×10^{-5} mol) of white prisms. HPLC (gradient mode): Identical to free ligand at $R_t \approx$ 21.0 min. MS (FAB/glycerol): m/z = 648 [M – $CF_3SO_3^-$]$^+$. $C_{29}H_{36}F_6MnN_6O_6S_2$ (797.14): calcd. C 43.67, H 4.55, N 10.54; found C 43.62, H 4.51, N 10.50.

[Mn(tach-6-MeOpyr)](CF$_3$SO$_3$)$_2$ (1e): A solution of $Mn(CF_3SO_3)_2{\cdot}6H_2O$ (0.058 g, 1.3×10^{-4} mol) in MeOH (2 mL) was mixed with a pale yellow solution of tach-6-MeOpyr (0.059 g, 1.2×10^{-4} mol) in MeOH (2 mL), giving a pale yellow solution. Addition of dry Et_2O (20 mL) to this solution gave a pale yellow oil that was isolated by decantation and triturated to a white powder with Et_2O (2 × 20 mL). The powder was dried under reduced pressure, then taken up in MeOH (3 mL) and subjected to vapor-phase diffusion of Et_2O to provide colorless prisms (**1e**·MeOH) suitable for X-ray diffraction. The prisms were isolated and dried under reduced pressure affording a 58% yield (0.059 g, 7.0×10^{-5} mol) of white prisms. μ_{eff} (DMSO, 25 °C) = 5.70 B.M. MS (FAB/gly): m/z = 696 [M – $CF_3SO_3^-$]$^+$, 532 [M –2 $CF_3SO_3^-$ – CH_3^+]$^+$. HPLC (gradient mode): identical to free ligand at R_t = 23.7 min. $C_{29}H_{36}F_6MnN_6O_9S_2$ (845.13): calcd. C 41.19, H 4.29, N 9.94; found C 41.03, H 4.33, N 9.86.

[Fe(tach-3-Mepyr)]Cl_2·1.5H_2O (2a·1.5H_2O): A pale green solution of $FeCl_2$·4H_2O (0.0070 g, 3.53 × 10^{-5} mol) in MeOH (1 mL) was added to a pale yellow solution of tach-3-Mepyr (0.0155 g, 3.48 × 10^{-5} mol) in MeOH (1 mL) producing a brown-yellow solution. Et_2O (2 mL) was added and the solution let stand for 48 h at 10 °C producing clusters of carmine red needles. Product was isolated and dried under reduced pressure affording deep red needles. ^{1}H NMR (400 MHz, [D_6]DMSO, 25 °C): δ = 7.59, 7.15, 6.91 (d, dd, d, 3 H, 3-MeC_5H_3N), 5.29 (br. t, 1 H, N*H*CH_2), 4.23, 4.02 (dd, dd, 2 H, NHC*H*$_2$py, diastereotopic), 2.95 (br. s, 1 H, cyclohexyl methine *H*), 2.37 (s, 3 H, C*H*$_3$py), 2.12 (br. d, 1 H, equatorial cyclohexyl methylene *H*), 1.84 (br. d, 1 H, axial cyclohexyl methylene *H*). $C_{27}H_{39}Cl_2FeN_6O_{1.5}$ (597.19): calcd. C 54.25, H 6.58, N 14.07; found C 54.17, H 6.22, N 13.76.

[Fe(tach-4-Mepyr)]Cl_2·1.5H_2O (2b·1.5H_2O): A pale green solution of $FeCl_2$·4H_2O (0.0110 g, 5.53 × 10^{-5} mol) in MeOH (1 mL) was added to a pale yellow solution of tach-4-Mepyr (0.0244 g, 5.49 × 10^{-5} mol) in MeOH (1 mL) affording a brown-yellow solution. Slow Et_2O diffusion produced several deep red microcrystals. The supernatant was decanted and the microcrystals were dried under reduced pressure. ^{1}H NMR (400 MHz, [D_6]DMSO, 25 °C): δ = 7.42, 7.17, 6.86 (s, d, d, 3 H, 4-MeC_5H_3N), 5.45 (br. t, 1 H, N*H*CH_2), 4.43, 4.19 (dd, dd, 2 H, NHC*H*$_2$py, diastereotopic), 3.21 (br. s, 1 H, cyclohexyl methine *H*), 2.37 (s, 3 H, C*H*$_3$py), 2.02 (br. d, 1 H, equatorial cyclohexyl methylene *H*), 1.79 (br. d, 1 H, axial cyclohexyl methylene *H*). $C_{27}H_{39}Cl_2FeN_6O_{1.5}$ (597.19): calcd. C 54.25, H 6.58, N 14.07; found C 54.56, H 6.16, N 13.86.

[Fe(tach-5-Mepyr)]Cl_2·H_2O (2c·H_2O): A pale green solution of $FeCl_2$·4H_2O (0.0108 g, 5.43 × 10^{-5} mol) in MeOH (1 mL) was added to a pale yellow solution of tach-5-Mepyr (0.0235 g, 5.28 × 10^{-5} mol) in MeOH (1 mL) creating a brown-yellow solution. Addition of Et_2O (ca. 20 mL) produced a slightly cloudy solution that yielded carmine red needles upon standing one week. The supernatant was decanted and the product was allowed to air dry giving deep red needles. ^{1}H NMR (400 MHz, [D_6]DMSO, 25 °C): δ = 7.65, 7.49, 6.78 (d, d, s, 3 H, 5-MeC_5H_3N), 5.57 (br. t, 1 H, N*H*CH_2), 4.43, 4.12 (dd, dd, 2 H, NHC*H*$_2$py), 3.13 (br. s, 1 H, cyclohexyl methine *H*), 2.08 (partially obscured) (s, 3 H, C*H*$_3$py), 2.09 (partially obscured) (br. d, 1 H, equatorial cyclohexyl methylene *H*), 1.81 (br. d, 1 H, axial cyclohexyl methylene *H*). $C_{27}H_{38}Cl_2FeN_6O$: calcd. (588.18) C 55.08, H 6.51, N 14.28; found C 54.73, H 6.45, N 13.88.

[Fe(tach-6-Mepyr)]$(ClO_4)_2$·H_2O (2d·H_2O): A yellow solution of $Fe(ClO_4)_2$·6H_2O (0.0160 g, 4.41 × 10^{-5} mol) in MeOH (1 mL) was added to a pale yellow solution of tach-6-Mepyr (19.5 g, 4.39 × 10^{-5} mol) in MeOH (1 mL) producing a dark red solution. During 24 h at 5 °C red needles precipitated from the solution. Removal of the supernatant and air-drying produced bright red needles. μ_{eff} (DMSO, 25 °C) = 5.46 B.M. at 25 °C. $C_{27}H_{38}Cl_2FeN_6O_9$ (716.14): calcd. C 45.24, H 5.35, N 11.73; found C 45.45, H 5.31, N 11.61.

[Fe(tach-6-MeOpyr)]Cl_2·1.5H_2O (2e·1.5H_2O): A pale green solution of $FeCl_2$·4H_2O (0.0113 g, 5.68 × 10^{-5} mol) in MeOH (1 mL) was added to a pale yellow solution of tach-6-MeOpyr (0.0276 g, 5.61 × 10^{-5} mol) in MeOH (1 mL) producing a yellow solution. Addition of ca. 15 mL of Et_2O produced a slightly cloudy solution that deposited yellow prisms upon standing 48 h. The supernatant was decanted and the product allowed to air-dry resulting in bright yellow prisms. μ_{eff} (DMSO, 25 °C) = 5.77 B.M. at 25 °C. $C_{27}H_{39}Cl_2FeN_6O_{4.5}$ (645.17): calcd. C 50.22, H 6.09, N 13.02; found C 50.21, H 6.10, N 12.84.

[Ni(tach-3-Mepyr)]$(ClO_4)_2$ (3a): A pale green solution of $Ni(ClO_4)_2$·6H_2O (0.0169 g, 4.62 × 10^{-5} mol) in MeOH (1 mL) was added to a pale yellow solution of tach-3-Mepyr (0.0204 g, 4.59 × 10^{-5} mol) in MeOH (1 mL) affording a pale purple-pink solution. Pink needles formed after 24 h. The supernatant was decanted and the solid was washed with Et_2O and dried, producing pale pink needles (0.0191 g, 59.3%). MS (ESI, MeOH): *m*/*z* = 501 = [M – 2 ClO_4^- – H^+], 601 [M – ClO_4^-]. $C_{27}H_{36}Cl_2N_6NiO_8$ (700.13): calcd. C 46.20, H 5.17, N 11.97; found C 46.43, H 5.28, N 12.06.

[Ni(tach-4-Mepyr)]$(ClO_4)_2$ (3b): A pale green solution of $Ni(ClO_4)_2$·6H_2O (0.0159 g, 4.35 × 10^{-5} mol) in MeOH (1 mL) was added to a pale yellow solution of tach-4-Mepyr (0.0197 g, 4.43 × 10^{-5} mol) in MeOH (1 mL) producing a pink solution. Small pink needles were produced by Et_2O diffusion into the MeOH solution. These crystals were isolated, washed with Et_2O, dried under reduced pressure, and taken up in MeOH (1 mL). Et_2O diffusion into the MeOH solution yielded pink needle clusters that were isolated and dried affording a pink solid (0.0184 g, 59.2%). MS (ESI, MeOH): *m*/*z* = 501 [M – 2 ClO_4^- – H^+], 601 [M – ClO_4^-]. $C_{27}H_{36}Cl_2N_6NiO_8$ (700.13): calcd. C 46.20, H 5.17, N 11.97; found C 46.31, H 5.14, N 11.94.

[Ni(tach-5-Mepyr)]$(ClO_4)_2$ (3c): A pale green solution of $Ni(ClO_4)_2$·6H_2O (0.0162 g, 4.42 × 10^{-5} mol) in MeOH (1 mL) was added to a pale yellow solution of tach-5-Mepyr (0.0200 g, 4.50 × 10^{-5} mol) in MeOH (1 mL) producing a purple-pink solution. Slow diffusion of Et_2O produced light pink microcrystals. The microcrystals were isolated, washed with Et_2O, dried under reduced pressure, and taken up in MeOH (1 mL). Diffusion of Et_2O into the MeOH solution produced pink needles that were isolated, washed with Et_2O, and dried producing pink needles (0.0221 g, 70.2%). MS (ESI, MeOH): *m*/*z* 501 [M – 2 ClO_4^- – H^+], 601 [M – ClO_4^-]. $C_{27}H_{36}Cl_2N_6NiO_8$ (700.13): calcd. C 46.20, H 5.17, N 11.97; found C 46.21, H 5.13, N 11.76.

[Ni(tach-6-Mepyr)]$(ClO_4)_2$·H_2O (3d·H_2O): A pale green solution of $Ni(ClO_4)_2$·6H_2O (0.0169 g, 4.62 × 10^{-5} mol) in MeOH (1 mL) was added to a pale yellow solution of tach-6-Mepyr (0.0203 g, 4.57 × 10^{-5} mol) in MeOH (1 mL) affording a dark yellow solution. Small light brown needles along with a yellow-brown oil formed after 24 h. The supernatant was decanted, the needles and oil were washed with Et_2O, and the needles were isolated and dried under vacuum (0.0046 g, 14%). MS (ESI, MeOH): *m*/*z* = 501 [M – 2 ClO_4^- – H^+], 601 [M – ClO_4^-]. μ_{eff} (DMSO, 25 °C) = 3.8 B.M. $C_{27}H_{38}Cl_2N_6NiO_9$ (718.14): calcd. C 45.03, H 5.32, N 11.65; found C 45.37, H 5.32, N 11.63.

[Ni(tach-6-Mepyr)]$(NO_3)_2$ (3d′): A pale yellow solution of tach-6-Mepyr (0.0839 g, 1.89 × 10^{-4} mol in MeOH, 2 mL) was added to a pale green solution of $Ni(NO_3)_2$·6H_2O (0.0549 g, 1.89 × 10^{-4} mol) in MeOH (2 mL) affording a peach solution. After adding Et_2O (12 mL) and standing for 2 h, pale lavender microcrystals formed which were isolated, washed with CH_3CN, and dried under reduced pressure to a pale violet solid. This was dissolved in MeOH followed by vapor diffusion of Et_2O, affording pale violet prisms of an ether adduct (**3d′**·0.5Et_2O) that were suitable for X-ray crystallography. These were isolated and dried to a pale violet solid (0.0828 g, 69.8%). MS (FAB/DMSO/NBA): *m*/*z* = 502 [M – 2 NO_3^-]. UV/Vis/NIR (MeOH): λ_{max} (ε) = 10800 (23.2), 12300 (13.7), 17800 cm^{-1} (7.8 cm^{-1} M^{-1}). μ_{eff} = 3.087 B.M. at 25 °C. $C_{27}H_{36}N_8NiO_6$ (626.21): calcd. C 51.35, H 5.80, N 17.83; found C 51.70, H 5.78, N 17.86.

[Ni(tach-6-MeOpyr)]$(ClO_4)_2$ (3e): A pale green solution of $Ni(ClO_4)_2$·6H_2O (0.0167 g, 4.57 × 10^{-5} mol) in MeOH (1 mL) was added to a pale yellow solution of tach-6-MeOpyr (0.0208 g, 4.23 × 10^{-5} mol) in MeOH (1 mL) producing a pale violet solution. The violet prisms that deposited after 24 h were isolated, washed with

Et_2O, and dried under vacuum (0.0150 g, 47.3%). MS (ESI, MeOH): *m/z* = 549 [M – 2 ClO_4^- – H^+], 649 [M – ClO_4^-]. μ_{eff} (DMSO, 25 °C) = 3.1 B.M. $C_{27}H_{36}Cl_2N_6NiO_{11}$ (748.12): calcd. C 43.25, H 4.84, N 11.21; found C 43.09, H 4.94, N 11.11.

[Cu(tach-3-Mepyr)](ClO$_4$)$_2$ (4a): A blue solution of $Cu(ClO_4)_2 \cdot 6H_2O$ (0.0267 g, 7.21 × 10^{-5} mol) in MeOH (1 mL) was added to a pale yellow solution of tach-3-Mepyr (0.0315 g, 7.09 × 10^{-5} mol) in MeOH (1 mL). A light indigo-blue precipitate formed that redissolved immediately to a blue solution. Slow Et_2O diffusion into the solution produced shiny blue prisms that were isolated and recrystallized from MeCN (4 mL) by vapor-phase diffusion of Et_2O (0.0419 g, 84.0%). MS (FAB/DMSO/MB): *m/z* = 606 [M – ClO_4^-]. UV/Vis/NIR (solid): λ_{max} = 14700 cm^{-1}. $C_{27}H_{36}Cl_2CuN_6O_8$ (705.13): calcd. C 45.86, H 5.13, N 11.89; found C 45.86, H 5.15, N 11.99.

[Cu(tach-4-Mepyr)](ClO$_4$)$_2$·H$_2$O (4b·H$_2$O): A blue solution of $Cu(ClO_4)_2 \cdot 6H_2O$ (0.0258 g, 6.96 × 10^{-5} mol) in MeOH (1 mL) was added to a pale yellow solution of tach-4-Mepyr (0.0310 g, 6.97 × 10^{-5} mol) in MeOH (1 mL). A blue precipitate formed that immediately redissolved to a blue solution. Slow Et_2O diffusion into the solution formed a blue oil which was triturated to a powder with Et_2O and recrystallized from MeOH by vapor-phase diffusion of Et_2O providing blue plates (0.0240 g, 48.8%). MS (FAB/DMSO/MB): *m/z* = 606 [M – ClO_4^-]. UV/Vis/NIR (solid): λ_{max} = 15100 cm^{-1}. $C_{27}H_{38}Cl_2CuN_6O_9$ (723.14): calcd. C 44.73, H 5.28, N 11.59; found C 44.64, H 5.10, N 11.19.

[Cu(tach-5-Mepyr)](ClO$_4$)$_2$ (4c): A blue solution of $Cu(ClO_4)_2 \cdot 6H_2O$ (0.0264 g, 7.12 × 10^{-5} mol) in MeOH (1 mL) was added to a pale yellow solution of tach-5-Mepyr (0.0322 g, 7.24 × 10^{-5} mol) in MeOH (1 mL). A light blue precipitate formed that immediately redissolved to a blue solution. Slow Et_2O diffusion into the solution formed a blue oil which was triturated to a powder with Et_2O and recrystallized from MeOH by vapor-phase diffusion of Et_2O providing blue needles (0.0376 g, 74.8%). MS (FAB/DMSO/MB): *m/z* = 606 [M – ClO_4^-]. UV/Vis/NIR (solid): λ_{max} = 15200 cm^{-1}. $C_{27}H_{36}Cl_2CuN_6O_8$ (705.13): calcd. C 45.86, H 5.13, N 11.89; found C 46.16, H 5.28, N 11.64.

[Cu(tach-6-MeOpyr)](ClO$_4$)$_2$ (4e): A blue solution of $Cu(ClO_4)_2 \cdot 6H_2O$ (0.0229 g, 6.18 × 10^{-5} mol) in MeOH (1 mL) was added to a pale yellow solution of tach-6-MeOpyr (0.0306 g, 6.22 × 10^{-5} mol) in MeOH (1 mL). A light blue precipitate formed that immediately redissolved to a blue solution. Slow Et_2O diffusion into the solution formed a blue oil which was triturated to a powder with Et_2O and recrystallized from MeCN (2 mL) by vapor-phase diffusion of Et_2O giving shiny blue needles suitable for X-ray crystallography (0.0365 g, 78.3%). MS (FAB/DMSO/MB): *m/z* = 654 [M – ClO_4^-], 493 (free tach-6-MeOpyr). UV/Vis/NIR (solid): λ_{max} = 10204, 15060 cm^{-1}. $C_{27}H_{36}Cl_2CuN_6O_{11}$ (753.11): calcd.C 42.95, H 4.81, N 11.13; found C 43.12, H 4.80, N 11.17.

[Zn(tach-3-Mepyr)](NO$_3$)$_2$·2H$_2$O (5a·2H$_2$O): A solution of $Zn(NO_3)_2 \cdot 6H_2O$ (0.0335 g, 1.126 × 10^{-4} mol) in MeOH (2 mL) was mixed with a pale yellow solution of tach-3-Mepyr (0.0502 g, 1.129 × 10^{-4} mol) in MeOH (2 mL) with no obvious change observed. Diffusion of Et_2O into the solution overnight gave clusters of colorless needles. The product was isolated, washed with Et_2O, and dried under reduced pressure affording white needles (0.0364 g, 5.74 × 10^{-5} mol, 51.0%). Suitable crystals for X-ray diffraction (shown to be **5a**·2MeOH·0.5H_2O) were grown from MeOH by vapor-phase diffusion of Et_2O. ^{1}H NMR (360 MHz, [D$_6$]DMSO, 25 °C): δ = 7.91, 7.76, 7.42 (d, d, dd, 3 H, 3-MeC_5H_3N), 4.41 (br. t, 1 H, N*H*CH_2), 4.05, 3.95 (dd, dd, 2 H, MepyCH_2N, diastereotopic), 3.29 (br. s, 1 H, cyclohexyl methine *H*), 2.32 (partially obscured) [s, 3 H, (CH_3)py], 2.34 (partially obscured) (br. d, 1 H, equatorial cyclohexyl methylene *H*), 1.88 (br. d, 1 H, axial cyclohexyl methylene *H*). MS (ESI): *m/z* = 507 [M – 2 NO_3^- – H^+], 570 [M – NO_3^-]. HPLC (gradient mode): R_t = 14.6 min (free ligand R_t = 22.9 min). $C_{27}H_{40}N_8O_8Zn$ (668.23): calcd. C 48.40, H 6.02, N 16.72; found C 48.15, H 6.06, N 16.66.

[Zn(tach-4-Mepyr)](NO$_3$)$_2$ (5b): A solution of $Zn(NO_3)_2 \cdot 6H_2O$ (0.0284 g, 6.16 × 10^{-5} mol) in MeOH (1 mL) was mixed with a pale yellow solution of tach-4-Mepyr (0.0278 g, 6.25 × 10^{-5} mol) in MeOH (1 mL), giving a pale yellow solution. Diffusion of Et_2O overnight gave colorless needle clusters. The product was isolated, washed with Et_2O, and dried under reduced pressure affording white needles (0.0235 g, 3.71 × 10^{-5} mol, 60.2%). ^{1}H NMR (360 MHz, [D$_6$]DMSO, 25 °C): δ = 7.68, 7.46, 7.34 (d, s, dd, 3 H, 4-MeC_5H_3N), 4.60 (br. t, 1 H, N*H*CH_2), 4.07 (m, 2 H, MepyCH_2N, diastereotopic), 3.26 (br. s, 1 H, cyclohexyl methine *H*), 2.48 (s, 3 H, CH_3py), 2.32 (br. d, 1 H, equatorial cyclohexyl methylene *H*), 1.86 (br. d, 1 H, axial cyclohexyl methylene *H*). MS (FAB/DMSO/MB): *m/z* = 507 [M – 2 NO_3^- – H^+], 570 [M – NO_3^-]. $C_{27}H_{36}N_8O_6Zn$ (632.20): calcd. C 51.15, H 5.72, N 17.68; found C 51.11, H 5.75, N 17.61.

[Zn(tach-5-Mepyr)](NO$_3$)$_2$·3H$_2$O (5c·3H$_2$O): A solution of $Zn(NO_3)_2 \cdot 6H_2O$ (0.0203 g, 6.82 × 10^{-5} mol) in MeOH (1 mL) was mixed with a pale yellow solution of tach-5-Mepyr (0.0301 g, 6.77 × 10^{-5} mol) in MeOH (1 mL), giving a colorless solution. Diffusion of Et_2O into the solution overnight gave a colorless oil. Trituration produced a white precipitate. The product was isolated, washed with Et_2O, and dried under reduced pressure affording a white powder (0.0345 g, 5.44 × 10^{-5} mol, 80.4%). ^{1}H NMR (360 MHz, [D$_6$]DMSO, 25 °C): δ = 7.95, 7.60, 7.52 (d, s, d, 3 H, 5-MeC_5H_3N), 4.59 (br. t, 1 H, N*H*CH_2), 4.07 (qd, 2 H, MepyCH_2N, diastereotopic), 3.23 (br. s, 1 H, cyclohexyl methine *H*), 2.29 (partially obscured) (s, 3 H, CH_3py), 2.33 (partially obscured) (br. d, 1 H, equatorial cyclohexyl methylene *H*), 1.86 (br. d, 1 H, axial cyclohexyl methylene *H*). MS (FAB/gly): *m/z* = 507 [M – 2 NO_3^- – H^+], 570 [M – NO_3^-]. $C_{27}H_{42}N_8O_9Zn$ (686.24): calcd. C 47.14, H 6.15, N 16.29; found C 47.18, H 6.11, N 15.96.

[Zn(tach-6-Mepyr)](NO$_3$)$_2$·H$_2$O (5d·H$_2$O): A solution of $Zn(NO_3)_2 \cdot 6H_2O$ (0.0423 g, 1.42 × 10^{-4} mol) in MeOH (2 mL) was mixed with a pale yellow solution of tach-6-Mepyr (0.0614 g, 1.38 × 10^{-4} mol) in MeOH (2 mL), giving a pale yellow solution. Adding Et_2O directly into the solution and waiting 18 h gave a white solid. The product was isolated, washed with Et_2O, and dried under reduced pressure affording a white solid (0.0143 g, 2.26 × 10^{-5} mol, 16.3%). ^{1}H NMR (360 MHz, [D$_6$]DMSO, 25 °C): δ = 7.89, 7.37, 7.31 (t, d, d, 3 H, 6-MeC_5H_3N), 4.23 (br. m, 1 H, N*H*CH_2), 4.20, 4.09 (d, d, 2 H, MePyCH_2N, diastereotopic), 3.08 (br. s, 1 H, cyclohexyl methine *H*), 2.16 (s, 3 H, C$H_3C_5H_3$N), 2.10 (br. d, 1 H, equatorial cyclohexyl methylene *H*), 1.82 (br. d, 1 H, axial cyclohexyl methylene *H*). MS (FAB/NBA/DMSO): *m/z* = 570 [M – NO_3^-], 507 [M – 2 NO_3^- – H^+]. HPLC (gradient): labile, identical to free tach-6-Mepyr at $R_t \approx$ 21.3 min. $C_{27}H_{38}N_8O_7Zn$ (650.22): calcd. C 49.74, H 5.87, N 17.19; found C 49.30, H 5.91, N 17.15.

[Zn(tach-6-Mepyr)](ClO$_4$)$_2$·H$_2$O (5d′·H$_2$O) and [Zn(tach-6-Mepyr)](ClO$_4$)$_2$·0.5MeOH·0.5H$_2$O (5d′·0.5MeOH·0.5H$_2$O): A pale yellow solution of tach-6-Mepyr (0.0540 g, 1.22 × 10^{-4} mol) in MeOH (4 mL) was added to a solution of $Zn(ClO_4)_2 \cdot 6H_2O$ (0.0493 g, 1.22 × 10^{-4} mol) in EtOH (4 mL) affording a white precipitate. After standing for 1 h, the precipitate was isolated and washed with Et_2O and MeOH. This was dried under reduced pressure affording a white solid in 60.3% yield (0.0569 g, 8.05 × 10^{-5} mol). Single crystals suitable for X-ray crystallography (shown to be

5d′·1/2MeOH·1/2H_2O) were obtained by Et_2O diffusion into an MeOH solution of the complex. ^1H NMR ([D_6]DMSO, 25 °C): δ = 7.89, 7.36, 7.34 (t, d, d, 3 H, $CH_3C_5H_3N$), 4.22, 4.05 (m, d, 3 H, diastereotopic methylene H's of MePyCH_2N and NHCH_2), 3.07 (br. s, cyclohexyl methine *H*), 2.15 (s, 3 H, CH_3C$_5$H$_3$N), 2.13 (br. d, 1 H, equatorial cyclohexyl methylene *H*), 1.82 (br. d, 1 H, axial cyclohexyl methylene *H*). MS (FAB/glycerol): *m*/*z* = 507 [M – 2 ClO_4^- – H^+]. $C_{27}H_{38}Cl_2N_6O_9Zn$(724.14): calcd. C 44.61, H 5.27, N 11.56; found C 44.58, H 5.41, N 11.74.

[Zn(tach-6-MeOpyr)](NO$_3$)$_2$ (5e): A solution of $Zn(NO_3)_2$·$6H_2O$ (0.0212 g, 7.13 × 10^{-5} mol) in MeOH (1 mL) was mixed with a colorless solution of tach-6-Mepyr (0.0364 g, 7.39 × 10^{-5} mol) in MeOH (1 mL) giving a colorless solution. Diffusion of Et_2O overnight produced colorless needles that were isolated, washed with Et_2O, and dried under reduced pressure affording white needles (0.0232 g, 3.36 × 10^{-5} mol, 47.1%). ^1H NMR (360 MHz, [D_6]DMSO, 25 °C): δ = 7.99, 7.10, 6.92 (t, d, d, 3 H, 6-OMeC$_5$H$_3$N), 4.39 (d, 1 H, NHCH_2), 4.14, 3.95 (dd, dd, 2 H, MeOpyCH_2N), 3.28 (s, 3 H, CH_3O), 3.13, (br. s, 1 H, cyclohexyl methine *H*), 2.24 (br. d, 1 H, equatorial cyclohexyl methylene *H*), 1.81 (br. d, 1 H, axial cyclohexyl methylene *H*). MS (FAB//NBA/DMSO): *m*/*z* = 618 [M – NO_3^-]. $C_{27}H_{36}N_8O_9Zn$ (680.19): calcd. C 47.56, H 5.32, N 16.43; found C 47.30, H 5.24, N 16.17.

[Zn(tachpyr)](CF$_3$SO$_3$)$_2$ (5f): A solution of $Zn(CF_3SO_3)_2$ (0.063 g, 1.7 × 10^{-4} mol) in MeOH (2 mL) was mixed with a pale yellow solution of tachpyr (0.070 g, 1.7 × 10^{-4} mol) in MeOH (2 mL), giving a pale yellow solution. Vapor-phase diffusion of Et_2O into this solution gave colorless needles after 18 h, which were isolated by decantation of solvent, washed with Et_2O and dried under reduced pressure affording an 82% yield (0.110 g, 1.4 × 10^{-4} mol) of white needles. ^1H NMR ([D_6]DMSO, 25 °C): MS (ESI, MeOH): *m*/*z* = 617 [M – $CF_3SO_3^-$], 469 [M – 2 $CF_3SO_3^-$ + H^+]$^+$. HPLC (gradient mode): R_t = 8.4 min (free ligand R_t = 18.8 min). HPLC (isocratic mode): R_t = 5.0 min. $C_{26}H_{30}F_6N_6O_6S_2Zn$ (764.09): calcd. C 40.76, H 3.95, N 10.97; found C 40.92, H 3.87, N 10.96.

Solution-Phase Complexation: Solution complexation studies for Fe^{II}, Ni^{II}, and Cu^{II} were carried out by combining aqueous or methanolic M^{II} and ligand solutions followed by spectroscopic analysis as described below; tach-*x*-Mepyr (*x* = 3, 4, 5 and 6) were easily dissolved in water while acidic conditions were required for tach-6-MeOpyr to dissolve (6 equiv. HCl). M^{II} (aq) was added to the chelator solution resulting in immediate complexation except in the case of tach-6-MeOpyr where 6 equiv. of NaOH was needed. Their spectra agreed well with those of the isolated metal complexes in MeCN (Table 1).

Fe^{II} Complexes: Complexation by tach-3-Mepyr and tach-6-Mepyr was studied in H_2O and solution reactions for all other chelators were run in MeOH. $FeCl_2$ (10 μL of 0.1 M aqueous) was added to tach-3-Mepyr (10 μL of 0.1 M aqueous) affording a bronze solution. Aqueous $FeCl_2$ (30 μL of 0.1 M) was added to tach-6-Mepyr (30 μL of 0.1 M) resulting in a red-brown solution. Each solution was brought to 1 mL with water producing solutions adequate for analysis. $FeCl_2$ (10 μL of 0.1 M methanolic solution) was added to tach-*x*-Mepyr or tach-6-MeOpyr (10 μL of 0.1 M methanolic solution) producing a bronze solution when *x* = 3, 4 or 5, a red-brown solution when *x* = 6 and a yellow solution for tach-6-MeOpyr. MeOH (980 μL) was added to the reactions producing solutions suitable for UV/Vis spectroscopic analysis.

Ni^{II} Complexes: Aqueous $NiCl_2$ (100 μL, 0.05 M) was added to aqueous tach-*x*-Mepyr or tach-6-MeOpyr, (100 μL of a 0.05 M solution) producing a clear pink solution with tach-*x*-Mepyr (*x* = 3, 4, 5), a clear yellow solution with tach-6-Mepyr, and a violet-white precipitate with tach-6-MeOpyr. Water (800 μL) was added to the reactions and the solutions were warmed (60 °C, 1 min) affording the appropriate pink, brown, and violet solutions for UV/Vis spectroscopic analysis.

Cu^{II} Complexes: All solution reactions for Cu^{II} complexes were run in water. $Cu(ClO_4)_2$ (60 μL of 0.05 M solution) was added to tach-*x*-Mepyr (*x* = 3, 4, 5) or tach-6-MeOpyr (120 μL of 0.025 M solution) producing a pale blue precipitate in all the reactions. Applying heat (50 °C, 30 s) and adding water (820 μL) produced bright blue solutions appropriate for analysis. Aqueous $Cu(ClO_4)_2$ (100 μL of 0.05 M solution) was added to aqueous tach-6-Mepyr (100 μL of 0.05 M solution) affording a pale blue precipitate. Water (800 μL) was added to the reaction producing a blue solution for UV/Vis spectroscopic analysis.

HPLC Studies: HPLC analyses of $[Fe(tach\text{-}3\text{-}Mepyr)]^{2+}$, $[Zn(tachpyr)]^{2+}$,[1] $[Zn(tach\text{-}6\text{-}Mepyr)]^{2+}$, $[Zn(tach\text{-}6\text{-}MeOpyr)]^{2+}$, $[Mn(tachpyr)]^{2+}$,[1] $[Mn(tach\text{-}6Mepyr)]^{2+}$ and $[Mn(tach\text{-}6MeOpyr)]^{2+}$ were conducted. Chromatograms in the gradient elution mode (RP-HPLC) were obtained with a Waters 600E/486/746 dual-pump system with UV detection at 254 nm. A Beckman Ultrasphere 4.6 × 25 cm RP-18 column was eluted with a gradient of 100% 0.05 M Et_3N·HOAc buffer (pH = 5.5) to 100% MeOH over 25 min. Chromatograms in the isocratic mode (RP-HPLC) were obtained on a Perkin–Elmer 250 dual-pump system with UV detection at 254 nm. A Beckman Ultrasphere 4.6 × 25 cm RP-18 column was eluted with 90% 0.05 M Et_3N·HOAc buffer (pH = 5.5) and 10% MeOH over 20 min. All complexes of tach-6-Mepyr and tach-6-MeOpyr, and also $[Mn(tachpyr)]^{2+}$, produced signals attributed to the free ligand and were therefore determined to be labile under gradient elution conditions. The complex $[Zn(tachpyr)]^{2+}$ was found inert as described previously,[1] and $[Fe(tach\text{-}3\text{-}Mepyr)]^{2+}$ showed a broad set of peaks indicative of imine formation previously observed for iron complexes of tach derivatives.[2,12] Under isocratic elution, the separation of $[Fe(tach\text{-}3\text{-}Mepyr)]^{2+}$ oxidation products improved sufficiently that the progressive transformations into higher imino species were observed.

Attempted Aqueous Reaction of tachpyr with Mg^{II} and Ca^{II}: These reactions were conducted in D_2O and analyzed by ^1H NMR spectroscopy; tachpyr (500 μL of 0.0241 M, 1.20 × 10^{-5} mol) was added to excess $MgBr_2$·$6H_2O$ (0.0180 g, 6.20 × 10^{-5} mol) or $CaCl_2$ (6.8 × 10^{-3} g, 6.1 × 10^{-5} mol); tachpyr remained unbound in both reactions.

X-ray Data Collection, Structure Solution and Refinement: See Tables 3 and 4) Single crystals of the various solvates of **1d**, **1e**, **3d**, **4e**, **5a**, and **5d′** were grown as described. The crystals were removed from the supernatant under a stream of N_2 and immediately covered with a layer of viscous hydrocarbon oil (Paratone N, Exxon). A suitable crystal was selected under the microscope, attached to a glass fiber, and immediately placed in the low-temperature nitrogen stream of the diffractometer. All data sets were collected using a Bruker SMART system, complete with 3-circle goniometer and CCD detector operating at –54 °C. The data sets were collected using a Cryojet low-temperature device from Oxford Instruments by employing graphite-monochromated Mo-K_α radiation (λ = 0.71073 Å). Crystal decay was monitored by repeating the initial frames at the end of the data collection and analyzing the duplicate reflections. In all cases, no decay was observed. The crystal structures of all compounds were solved by direct methods, as included in the SHELX program package.[13] Absorption corrections were made with SADABS.[14] Missing atoms were located in subsequent difference Fourier maps and included in the refinement. The structures were refined by full-matrix least-squares refinement on F^2.

Hydrogen atoms were placed geometrically and refined using a riding model, including free rotation about C–C bonds for methyl groups. Thermal parameters for hydrogen atoms were refined with U_{iso} constrained at 1.2 (for non-methyl groups), and 1.5 (for methyl groups) times U_{eq} of the carrier C atom. All non-hydrogen atoms, with the exception of some disordered or restrained positions were refined anisotropically. The twist angles Φ were calculated by first determining the centroid in each of the triangles of the three cyclohexylamino nitrogen atoms [N(tach); designated as X1] and of the three ethylamino nitrogen atoms [N(en); designated as X2]. Then, the torsion angles N(tach)–X1–X2–N(en), each involving the two nitrogen atoms of the same chelate arm, were calculated and averaged. ORTEP drawings were made with SHELXTL[13] and ORTEP-3.[15,16] The ORTEP plots of **1d**·1/2H_2O·1/2MeOH and **1e** are available as Supporting Information. CIF files for the structural analyses of **1d**·1/2H_2O·1/2MeOH, **1e**, **3d′**·0.5Et_2O, **4e**, **5a**·2MeOH·0.5H_2O, and **5d′**·0.5H_2O·0.5MeOH have been deposited with the Cambridge Crystallographic Data Centre. CCDC-

Table 3. Crystal data and structure refinement parameters for **1d**·0.5H_2O·0.5MeOH, **1e**·MeOH and **3d′**·0.5Et_2O.

	1d·0.5H_2O·0.5MeOH	**1e**·MeOH	**3d′**·0.5Et_2O
Empirical formula	$C_{27.50}H_{37.50}Cl_2MnN_6O_9$	$C_{30}H_{39}F_6MnN_6O_{10}S_2$	$C_{29}H_{41}N_8NiO_{6.50}$
Formula mass	721.97	876.73	664.41
Crystal system	triclinic	monoclinic	monoclinic
Space group	$P\bar{1}$	$P2_1/c$	$P2_1/n$
a [Å]	9.4981(4)	14.490(8)	12.0745(4)
b [Å]	17.6530(7)	15.655(8)	16.6907(5)
c [Å]	19.2146(7)	17.015(9)	15.0261(5)
α [°]	96.521(3)	90	90
β [°]	95.382(1)	104.461(10)	92.280(1)
γ [°]	94.633(1)	90	90
V [Å^3]	3173.1(2)	3737(3)	3025.8(2)
Z	4	4	4
Color	colorless	colorless	pale violet
Crystal shape	fragment	fragment	fragment
Crystal dimensions [mm]	0.14 × 0.20 × 0.27	0.05 × 0.12 × 0.21	0.24 × 0.35 × 0.40
$D_{calcd.}$ [g cm^{-3}]	1.515	1.558	1.458
μ [mm^{-1}]	0.646	0.557	0.700
Λ [Å]	0.71073	0.71073	0.71073
Refl. collected/unique	20018/8601	16755/4080	18825/3830
θ range [°]	1.07–27.88	1.79–23.29	1.82–27.88
Parameters	883	512	419
GOF	0.996	1.040	1.054
Final R indices [$I > 2\sigma(I)$]	R = 0.0625	R = 0.0343	R = 0.0710
	R_w = 0.1518	R_w = 0.0898	R_w = 0.1473
$\Delta\rho_{max.}$ [e·Å^{-3}]	1.601	0.552	0.715

Table 4. Crystal data and structure refinement parameters for **4e**, **5a**·2MeOH·0.5H_2O and **5d′**·0.5H_2O·0.5MeOH.

	4e	**5a**·2MeOH·0.5H_2O	**5d′**·0.5H_2O·0.5MeOH
Empirical formula	$C_{27}H_{36}Cl_2CuN_6O_{11}$	$C_{58}H_{72}N_{16}O_{17}Zn_2$	$C_{55}H_{72}Cl_4N_{12}O_{18}Zn_2$
Formula mass	755.06	1396.06	730.91
Crystal system	monoclinic	monoclinic	triclinic
Space group	$P2_1/n$	$P2_1/c$	$P\bar{1}$
a [Å]	20.450(4)	16.3245(10)	9.4081(4)
b [Å]	16.643(4)	18.9702(12)	17.6239(8)
c [Å]	21.223(5)	20.9807(13)	19.1521(8)
α [°]	90	90	96.581(1)
β [°]	118.293(4)	92.3000(10)	95.722(1)
γ [°]	90	90	95.383(1)
V [Å^3]	6360(2)	6492.0(7)	3121.1(2)
Z	8	4	2
Color	blue	colorless	colorless
Crystal shape	fragment	needle	fragment
Crystal dimensions [mm]	0.03 × 0.09 × 0.31	0.30 × 0.30 × 0.55	0.06 × 0.08 × 0.49
$D_{calcd.}$ [g cm^{-3}]	1.577	1.428	1.563
μ [mm^{-1}]	0.924	0.819	1.021
Λ [Å]	0.71073	0.71073	0.71073
Refl. collected/unique	28509/5763	34815/8774	19752/7146
θ range [°]	1.14–23.29	1.45–25.00	1.08–27.97
Parameters	868	839	883
GOF	0.813	1.022	1.027
Final R indices [$I > 2\sigma(I)$]	R = 0.0378	R = 0.0538	R = 0.0698
	R_w = 0.0812	R_w = 0.1427	R_w = 0.1346
$\Delta\rho_{max.}$ [e·Å^{-3}]	0.704	1.499	0.986

268824 to -268829 contain the supplementary crystallographic data for this paper. These data can be obtained free of charge from The Cambridge Crystallographic Data Centre via www.ccdc.cam.ac.uk/data_request/cif.

Cytotoxicity Assays: MCF-7, a breast cancer cell line, was obtained from the ATCC and was grown in Dulbecco's Modified Eagle medium containing 10% fetal bovine serum in a humidified chamber containing 5% CO_2. 5×10^3 cells were plated in 96-well tissue culture dishes and allowed to attach overnight before test compounds were added. Six replicate cultures were used for each point. After 8, 24, 48 and 72 h (8 and 72 h in the case of tach-6-Mepyr), viability was assessed using an MTT assay, in which 3-(4,5-dimethylthiazol-2-yl)-2,5-diphenyltetrazolium bromide was added to the medium and the formation of a reduced product assayed by measuring the optical density at 560/650 nm after 3 h. Color formation is proportional to viable cell number.[17] Assays of all compounds were repeated at least three times.

Acknowledgments

We thank the NIH for the support of this work (Grant DK-57781-R01 to S. V. T.). Research at The University of Alabama is supported by the Division of Chemical Sciences, Office of Basic Energy Sciences, Office of Research, U. S. Department of Energy (Grant DE-FG02-96ER14673). Purchase of the X-ray equipment at Syracuse University was made possible with generous support from the National Science Foundation (CHE-95-27898), Syracuse University and the W. M. Keck Foundation.

[1] G. Park, A. M. Przyborowska, N. Ye, N. Tsoupas, C. B. Bauer, G. A. Broker, R. D. Rogers, M. W. Brechbiel, R. P. Planalp, *Dalton Trans.* **2003**, 318.
[2] G. Park, F. Lu, N. Ye, M. Brechbiel, S. Torti, F. Torti, R. Planalp, *J. Biol. Inorg. Chem.* **1998**, *3*, 449.
[3] G. Park, E. Dadachova, A. Przyborowska, S.-J. Lai, D. Ma, G. Broker, R. Rogers, R. Planalp, M. Brechbiel, *Polyhedron* **2001**, *20*, 3155.
[4] G. Park, N. Ye, R. Rogers, M. Brechbiel, R. Planalp, *Polyhedron* **2000**, *19*, 1155.
[5] S. V. Torti, R. P. Planalp, M. W. Brechbiel, G. Park, F. M. Torti, in: *Molecular Biology of Hematopoiesis* (Ed.: N. G. Abraham), Kluwer/Plenum Press, New York, **1999**, vol. 6 , pp. 381.
[6] N. Le, D. Richardson, *Biochim. Biophys. Acta* **2002**, *1603*, 31.
[7] J. Easmon, *Expert Opin. Ther. Pat.* **2002**, *12*, 789.
[8] S. V. Torti, F. M. Torti, S. P. Whitman, M. W. Brechbiel, G. Park, R. P. Planalp, *Blood* **1998**, *92*, 1384.
[9] R. Zhao, R. P. Planalp, R. Ma, B. Greene, B. Jones, M. Brechbiel, F. M. Torti, S. V. Torti, *Biochem. Pharmacol.* **2004**, *67*, 1677.
[10] D. Ma, F. Lu, T. Overstreet, D. E. Milenic, M. W. Brechbiel, *Nucl. Med. Biol.* **2002**, *29*, 91.
[11] D. F. Evans, *J. Chem. Soc.* **1959**, 2003.
[12] G. Lu, D. P. Kennedy, S. Lai, G. Park, A. M. Przyborowska, M. W. Brechbiel, G. A. Broker, R. D. Rogers, R. Ma, F. M. Torti, S. V. Torti, R. P. Planalp, *Inorg. Chem.*, submitted for publication.
[13] G. M. Sheldrick, *SHELXTL*, version 5.05, Siemens Analytical X-ray Instruments Inc., **1996**.
[14] G. M. Sheldrick, *Program for Semiempirical Absorption Correction of Area Detector Data*, University of Göttingen, Germany, **1996**.
[15] M. Burkitt, *Methods Enzymol.* **1994**, *234*, 66.
[16] L. J. Farrugia, *J. Appl. Crystallogr.* **1997**, *30*, 565.
[17] T. Mosmann, *J. Immunol. Methods* **1983**, *65*, 55.
[18] K. A. Hilfiker, R. D. Rogers, M. W. Brechbiel, R. P. Planalp, *Inorg. Chem.* **1997**, *36*, 4600.
[19] H. L. Chum, J. A. Vanin, M. I. D. Holanda, *Inorg. Chem.* **1982**, *21*, 1146.
[20] H. Toftlund, S. Yde-Andersen, *Acta Chem. Scand., Series A* **1981**, *35*, 575.
[21] K. Wieghardt, E. Schoeffmann, B. Nuber, J. Weiss, *Inorg. Chem.* **1986**, *25*, 4877.
[22] L. J. Wilson, D. Georges, M. A. Hoselton, *Inorg. Chem.* **1975**, *14*, 2968.
[23] R. D. Hancock, G. J. McDougall, *J. Chem. Soc. Dalton Trans.* **1977**, 67.
[24] G. Park, J. Shao, F. H. Lu, R. D. Rogers, N. D. Chasteen, M. W. Brechbiel, R. P. Planalp, *Inorg. Chem.* **2001**, *40*, 4167.
[25] M. Duggan, N. Ray, B. Hathaway, G. Tomlinson, P. Brint, K. Pelin, *J. Chem. Soc. Dalton Trans.* **1980**, 1342.
[26] K. D. Karlin, J. C. Hayes, S. Juen, J. P. Hutchinson, J. Zubieta, *Inorg. Chem.* **1982**, *21*, 4106.
[27] B. Figgis, *Introduction to ligand fields*, Wiley, New York, **1966**.
[28] R. D. Shannon, C. T. Prewitt, *Acta Crystallogr. Sect. B* **1969**, *25*, 925.
[29] R. Shannon, *Acta Crystallogr., Sect. A* **1976**, *32*, 751.
[30] B. Hathaway, R. Gillard, J. McCleverty, in: *Comprehensive Coordination Chemistry* (Eds.: G. Wilkinson, R. Gillard, J. McCleverty), Pergamon, Oxford, **1987**, vol. 5, chapter 53.4.

Received: April 28, 2005
Published Online: August 24, 2005

